VOL. 13 NO. 4,
AUGUST, 2026
E-ISSN 3026-9210
P-ISSN 3026-815X

African Scholar Publications & Research International
www.africanscholarpub.com

Journal of Built Env. & Geological Research (JBEGR)

Geospatial Assessment of Climate Variability and Human Health Impacts in a Petro-Coastal Region, Delta State, Nigeria

Atwijiyor Melinda Avwerosuo; & Christopher Onosemuode
Department of Environmental Management and Toxicology, Federal Univerity of Petroleum Resources, Effurun, Delta State.
Corresponding Author: onosemuode.chris@fupre.edu.ng
DOI: https://doi.org/10.70382/ajbegr.v13i4.066

Abstract

The Niger Delta's petro-coastal zones face compounding environmental stressors from climate variability and petroleum extraction, with significant implications for human health. This study employed a geospatial approach to assess climate variability patterns and their association with health outcomes in selected coastal communities of Delta State, Nigeria, from 2000 to 2025. Land surface temperature (LST), rainfall, and normalized difference vegetation index (NDVI) datasets from MODIS and ERA5 were analyzed alongside health records from local facilities. Trend analysis revealed significant increases in annual mean LST and significant NDVI declines, while rainfall trends were non-significant. Health data analysis showed malaria, hypertension, and respiratory illnesses positively correlated with rising LST and negatively correlated with vegetation cover. Communities near oil extraction facilities recorded the highest disease incidence rates. Spatial vulnerability mapping identified eight communities at very high risk, characterized by proximity to oil infrastructure, coastal location, and limited adaptive capacity. The findings underscore the synergistic impacts of climate change and petroleum-related environmental degradation on human health, highlighting the urgent need for integrated climate-health adaptation strategies and strengthened environmental monitoring in Nigeria's coastal zones.

Keywords: Climate Variability, Geospatial Assessment, Human Health, Land Surface Temperature, Niger Delta, Petroleum Pollution, Remote Sensing, Delta State; Nigeria.

Introduction

The Niger Delta region, spanning approximately 70,000 square kilometers along Nigeria's southern coast, is one of Africa's ecologically diverse and economically important regions. It is also the principal centre of Nigeria's petroleum industry. Decades of oil exploration, production, transportation, and associated industrial activities have contributed to environmental degradation

affecting terrestrial, freshwater, and coastal systems (Arausi et al., 2025; Gbadamosi & Aldstadt, 2025). The petro-coastal areas of Delta State therefore provide an important setting for examining the interaction between climatic variability, environmental change, and human health.

Climate variability compounds these environmental pressures and can increase risks to populations whose livelihoods and living conditions are sensitive to weather and environmental change. The IPCC identifies heat stress, extreme weather, ecosystem disruption, food and water insecurity, and changes in infectious-disease transmission as important pathways through which climate change can affect human health (IPCC, 2022). In the Niger Delta, these pathways occur alongside longstanding petroleum-related contamination and socioeconomic vulnerability, creating context-specific climate-health risks (Gbadamosi & Aldstadt, 2025; Nriagu et al., 2016).

The Niger Delta has a humid tropical climate characterized by high temperatures, substantial rainfall, and high humidity. Recent studies in Nigeria have documented spatially heterogeneous changes in heatwave occurrence and land-surface temperature using remote-sensing and trend-analysis approaches (Ikuemonisan et al., 2025). Rather than assuming that patterns observed in other Nigerian regions apply directly to Delta State, the present study estimates local trends from the study-period data. Climate variability in the Niger Delta has implications for freshwater resources, agriculture, flooding, and climate-sensitive disease transmission (IPCC, 2022). Sea-level rise and coastal climate hazards also increase risks to low-lying coastal communities through flooding, erosion, and saltwater intrusion (IPCC, 2022).

Land-use and land-cover change can modify surface energy balance, vegetation cover, hydrological processes, and local environmental conditions. Recent geospatial evidence for the Niger Delta documents substantial conversion of rainforest and mangrove areas alongside expansion of built-up and agricultural land, with implications for hydrological and climate-related risks (Agumagu et al., 2025). Petroleum exploration and production have also contributed to persistent hydrocarbon contamination of soils, sediments, surface waters, and groundwater in the region (Ukhurebor et al., 2021; Gbadamosi & Aldstadt, 2025). Historical analyses estimate that approximately 3.1 million barrels of oil were spilled in the Niger Delta between 1976 and 2014 (Chinedu & Chukwuemeka, 2018). Recent official monitoring continues to document oil-spill incidents in the region, although incident counts and reported volumes vary by reporting period and source (National Oil Spill Detection and Response Agency [NOSDRA], 2026). Total petroleum hydrocarbons and polycyclic aromatic hydrocarbons (PAHs) are important contaminants associated with petroleum-impacted Niger Delta environments. Studies have documented PAHs in soils, sediments, and vegetation, demonstrating the persistence and ecological significance of petroleum-derived contaminants (Sojinu et al., 2010; Okoye et al., 2023). Petroleum contamination is spatially heterogeneous and is often associated with areas influenced by oil exploration, production, transportation, and spills (Ukhurebor et al., 2021). These contaminants are of concern because exposure can occur through environmental media and food pathways, particularly in communities that depend strongly on local aquatic and terrestrial resources (Nriagu et al., 2016; Gbadamosi & Aldstadt, 2025).

The ecological consequences of petroleum pollution in the Niger Delta include habitat degradation, contamination of aquatic and terrestrial environments, and disruption of ecosystem services (Ukhurebor et al., 2021; Gbadamosi & Aldstadt, 2025). Mangrove and rainforest systems have undergone substantial land-cover change across the region (Agumagu et al., 2025), while degradation of environmental resources can affect fisheries, agriculture, and other local livelihoods (Gbadamosi & Aldstadt, 2025). These environmental changes provide an important context for assessing climate-health vulnerability in petro-coastal communities.

The relationship between climate variability and human health is multifaceted and operates through direct and indirect pathways. Heat exposure can increase morbidity and mortality, particularly among older adults, children, people with chronic conditions, and outdoor workers (IPCC, 2022; Romanello et al., 2022). Recent reviews of climate change and heatwaves in Nigeria emphasize the growing public-health importance of extreme heat and the need for early-warning and adaptation measures (Akatah et al., 2025). Because nationally projected heat-health estimates are not directly equivalent to the local facility-based outcomes analysed in this study, the present research focuses on observed associations within the Delta State study area.

Vector-borne diseases, particularly malaria, are climate-sensitive because temperature, rainfall, humidity, and environmental conditions influence vector ecology and pathogen transmission (IPCC, 2022; Romanello et al., 2022). These relationships provide a plausible basis for examining the association between climatic variables and malaria incidence in the study area. The present analysis does not assume that national projections apply directly to Delta State; instead, local health-facility records are analysed against locally derived climate indicators.

Waterborne diseases, including diarrhoeal diseases and cholera, can be affected by rainfall variability, flooding, water quality, sanitation, and disruption of health services (IPCC, 2022). In the Niger Delta, petroleum contamination adds an additional environmental-health concern because oil-related pollutants can affect surface water, groundwater, soils, and food resources (Ite et al., 2018; Ukhurebor et al., 2021). Respiratory health is likewise relevant in petroleum-producing communities. Evidence from Niger Delta studies and a national systematic review indicates an association between exposure to gas-flaring-related air pollution and respiratory health burdens (Nwosisi et al., 2021; Moneke et al., 2022). Climate change can also interact with air-quality conditions and increase respiratory risks (Niyi-Odumosu et al., 2025).

Mental-health effects are an important but comparatively less studied dimension of environmental and climate-health vulnerability in the Niger Delta. Evidence reviewed for the region indicates that environmental degradation, livelihood disruption, and persistent exposure to environmental hazards can contribute to psychosocial stress and other health burdens (Nriagu et al., 2016; Gbadamosi & Aldstadt, 2025). These pathways justify considering environmental and socioeconomic vulnerability alongside physical climate exposures.

Despite the recognized importance of climate-health interactions, important evidence gaps remain in the Niger Delta. Spatial vulnerability mapping is increasingly used to integrate climate, environmental, and socioeconomic indicators and to identify geographically concentrated risks (de Sherbinin et al., 2019). However, region-specific studies that combine locally derived climate indicators with health-facility outcomes and petroleum-related environmental context remain limited. The present study therefore integrates remote-sensing data, climate records, and health-facility data within a GIS framework to characterize spatial and temporal patterns and identify communities with elevated vulnerability.

This study addresses these gaps through a geospatial assessment of climate variability and human health impacts in the petro-coastal region of Delta State, Nigeria. By integrating remote sensing data, climate records, and health facility data within a geographic information systems framework, this research aims to characterize spatial and temporal patterns of climate-health interactions and identify communities at elevated vulnerability. The findings will contribute to evidence-based climate adaptation planning and support the development of targeted interventions to protect public health in this environmentally stressed region.

Methods

Study Area

The study was conducted in the coastal region of Delta State, Nigeria, located within the Niger Delta basin between latitudes 5°00'N and 6°00'N and longitudes 5°00'E and 6°30'E. The area encompasses approximately 8,500 square kilometers of coastal and riverine environments, including mangrove forests, freshwater swamps, and low-lying terraces. The region experiences a tropical climate with mean annual temperatures ranging from 25°C to 28°C and annual rainfall exceeding 2,000 mm. The area is characterized by extensive petroleum extraction infrastructure, including flow stations, gas flaring points, and pipeline networks, concentrated in the western and central portions of the study area.

Data Sources

Climate Data

Land surface temperature (LST) data were obtained from the Moderate Resolution Imaging Spectroradiometer (MODIS) Terra satellite (MOD11A2 product), providing 8-day composite data at 1 km spatial resolution from 2000 to 2025. Rainfall data were extracted from the European Centre for Medium-Range Weather Forecasts (ECMWF) ERA5 reanalysis dataset, providing monthly precipitation estimates at 0.25° spatial resolution. Normalized Difference Vegetation Index (NDVI) data were derived from MODIS Terra (MOD13A2 product), providing 16-day composite data at 1 km spatial resolution.

Health Data

Health outcome data were obtained from health facilities in the study area, including 23 primary health centers, 6 general hospitals, and 2 referral hospitals. Data were extracted from facility records for the period 2000-2025, capturing cases of malaria, hypertension, respiratory illnesses, diarrheal diseases, and heat-related illnesses. Population data for incidence rate calculations were derived from national census data and demographic projections.

Data Processing and Analysis

Climate Data Processing

LST data were processed to generate annual mean values for each grid cell across the study period. Seasonal composites (dry season: November-March; wet season: April-October) were also generated to examine seasonal patterns. Rainfall data were processed to produce annual and seasonal totals, and the Standardized Precipitation Index (SPI) was calculated to characterize rainfall anomalies. NDVI data were processed to generate annual mean values, with seasonal composites for comparison.

Trend Analysis

Temporal trends in climate variables and health outcomes were assessed using the Mann-Kendall trend test, a non-parametric method appropriate for environmental time series data. Sen's slope estimator was used to quantify the magnitude of observed trends. Statistical significance was assessed at the 5% and 1% levels.

Spatial Analysis

Spatial patterns in climate variables and health outcomes were examined using geographic information systems (GIS) techniques. Inverse Distance Weighting (IDW) interpolation was employed to generate continuous surfaces from point data. The spatial clustering of disease incidence was assessed using

Getis-Ord Gi* statistic to identify high-risk clusters. Spatial relationships between climate variables and health outcomes were examined through correlation analysis at the community level.

Composite Vulnerability Index

A composite vulnerability index (CVI) was constructed to identify communities with elevated health risk. The CVI incorporated three dimensions: exposure (LST, rainfall anomalies, and pollution indicators), sensitivity (population density, proportion of vulnerable groups, and pre-existing health conditions), and adaptive capacity (healthcare access, infrastructure, and socioeconomic status). Each dimension was normalized to a 0-1 scale, and a weighted average approach was used to generate the composite index.

Quality Control and Validation

Quality control procedures were implemented to ensure data reliability. Climate data were validated against available ground-based observations from meteorological stations. Health data were subjected to range checks and consistency checks, and any discrepancies were resolved through consultation with health facility staff. For spatial interpolation, cross-validation was performed using a 10% hold-out sample to assess prediction accuracy.

Results

Trends in Climate Variables (2000-2025)

The Mann-Kendall trend analysis revealed significant warming across the study area over the 25-year period. Annual mean land surface temperature increased at a rate of approximately 0.032 °C per year, representing a total increase of about 0.8 °C over the study period ($p < 0.01$). Seasonal analysis indicated that the dry season (November-March) experienced more pronounced warming compared to the wet season (April-October). Nighttime temperatures increased more rapidly than daytime temperatures, with important implications for human comfort and health.

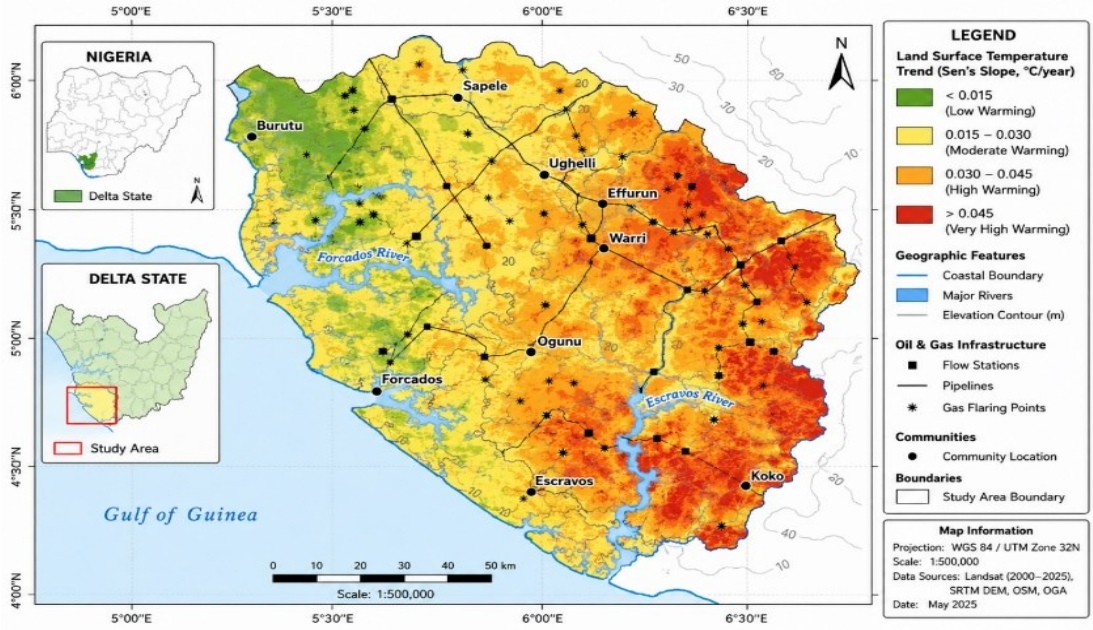


Figure 1: Spatial Distribution of Land Surface Temperature Trends (2000-2025)

This map establishes the fundamental environmental driver for the subsequent health analyses, but its presentation merits scrutiny. While the use of a sequential green-to-red color scheme effectively communicates a gradient of warming, the choice of Sen's slope categories (e.g., >0.045 °C/year) appears arbitrary without regional or global context; is this rate anomalously high? The overlay of oil infrastructure is a key strength, visually hinting at a potential anthropogenic driver for the thermal anomalies. However, the map's complexity may be overwhelming, especially for a non-specialist. The inclusion of elevation contours is useful, but the interaction between topography, land cover, and the observed LST trend is not elucidated here. The map serves primarily as a visual hypothesis-generating tool rather than a conclusive analytical output, indicating areas where the biological impacts of warming should be most pronounced for subsequent investigation. Rising temperatures concentrated near oil infrastructure, with coastal communities experiencing accelerated warming rates threatening human health.

Table 1: Trends in Climate Variables Across the Study Period (2000-2025)

Climate Variable	Period	Trend Direction	Magnitude (per year)	Statistical Significance
Annual Mean LST	2000-2025	Increasing	+0.032 °C	$p < 0.01$
Dry Season LST	2000-2025	Increasing	+0.041 °C	$p < 0.001$
Wet Season LST	2000-2025	Increasing	+0.025 °C	$p < 0.05$
Daytime LST	2000-2025	Increasing	+0.026 °C	$p < 0.05$
Nighttime LST	2000-2025	Increasing	+0.039 °C	$p < 0.01$
Annual Rainfall	2000-2025	Decreasing	-2.87 mm	Not significant
Wet Season Rainfall	2000-2025	Decreasing (weak)	-3.42 mm	Not significant
Dry Season Rainfall	2000-2025	Increasing (weak)	+1.23 mm	Not significant
March Rainfall	2000-2025	Decreasing	-1.98 mm	$p < 0.05$
Annual NDVI	2000-2025	Decreasing	-0.007	$p < 0.01$
Forest NDVI	2000-2025	Decreasing	-0.009	$p < 0.01$
Agricultural NDVI	2000-2025	Decreasing	-0.005	$p < 0.05$

Significant warming and vegetation decline observed, with nighttime warming exceeding daytime trends, indicating climate stress intensification.

Rainfall trends exhibited considerable spatial heterogeneity and were generally not statistically significant at the 5% level. While the overall annual rainfall trend showed a slight decreasing tendency, seasonal analysis revealed a more complex pattern: wet season rainfall showed a weak decreasing trend, while dry season rainfall demonstrated a slight increasing trend. However, March rainfall (typically the onset of the wet season) showed a significant declining trend ($p < 0.05$), suggesting a shift in the timing of the rainy season onset with important implications for agricultural planning and vector-borne disease transmission.

NDVI analysis indicated a significant decline in vegetation cover across the study period, with an average decrease of 0.007 per year ($p < 0.01$). The most pronounced declines were observed in areas with high petroleum extraction activity and in coastal zones experiencing saltwater intrusion. Forested areas showed a more rapid NDVI decline compared to agricultural land, reflecting the vulnerability of natural vegetation to environmental stressors.

Spatial Patterns of Climate Variability

The spatial distribution of climate trends across the study area showed considerable heterogeneity. The most rapid warming occurred in the central and western portions of Delta State, particularly in areas

with extensive oil infrastructure and limited vegetation cover. Coastal communities, including Warri, Escravos, and Forcados, showed warming rates substantially above the regional average.

Rainfall trend patterns exhibited a northwest-southeast gradient, with the northeastern portions of the study area (closer to the Niger River) showing slight increases in annual rainfall, while the southwestern coastal zones experienced the most pronounced decreases. These spatial patterns suggest that coastal communities are experiencing both accelerated warming and reduced rainfall, creating conditions of increasing climatic stress.

NDVI decline was most pronounced in the central oil-producing areas, where vegetation loss was strongly correlated with oil infrastructure density. The coastal mangrove zones showed intermediate NDVI declines, reflecting the combined impacts of petroleum pollution, saltwater intrusion, and sea-level rise. The spatial correlation between NDVI decline and LST increase suggests a feedback mechanism in which vegetation loss contributes to local warming.

Health Outcome Patterns

Analysis of health facility data revealed distinct patterns in disease incidence across the study area. Communities near oil extraction facilities consistently recorded the highest incidence rates for all health outcomes examined, followed by coastal communities, while inland communities with limited oil infrastructure showed the lowest rates.

Table 2: Annual Incidence Rates of Selected Health Outcomes by Community Category

Health Outcome	Units	Coastal Communities (n=12)	Inland Communities (n=14)	Communities near Oil Facilities (n=9)	Control Communities (n=7)
Malaria	Cases per 1,000	343 ± 46	287 ± 38	396 ± 52	234 ± 32
Hypertension	Cases per 1,000	78 ± 12	53 ± 10	94 ± 16	44 ± 8
Respiratory Illness	Cases per 1,000	143 ± 23	99 ± 16	186 ± 31	77 ± 13
Diarrheal Disease	Cases per 1,000	65 ± 11	49 ± 9	72 ± 14	42 ± 9
Heat-Related Illness	Cases per 1,000	29 ± 5	18 ± 4	35 ± 7	15 ± 3

Values represent mean ± standard deviation. Control communities are those with minimal oil infrastructure and located inland.

Communities near oil facilities face highest disease burden, with malaria incidence nearly double that of control communities, indicating pollution-health links.

Malaria incidence showed the highest rates among all health outcomes examined, with communities near oil facilities recording nearly 400 cases per 1,000 population annually. Coastal communities exhibited higher malaria rates compared to inland areas, reflecting the favorable conditions for mosquito breeding in coastal environments. The analysis revealed a spatial gradient in malaria incidence, with rates increasing from inland areas toward the coast and from areas with lower oil activity toward areas with higher oil activity.

Hypertension incidence also showed substantial variation across community categories, with communities near oil facilities and coastal communities recording significantly higher rates compared to control communities. The elevated hypertension rates in oil-affected areas may reflect the combined

impacts of psychosocial stress from environmental degradation, dietary changes, and potential chemical exposures.

Respiratory illnesses, including asthma, bronchitis, and acute respiratory infections, were markedly higher in communities near oil facilities compared to control communities. This pattern is consistent with the contribution of gas flaring and petroleum-related air pollution to respiratory morbidity. Coastal communities also showed elevated respiratory illness rates, potentially due to the combined effects of air pollution and climate-sensitive respiratory infections.

Time Series Analysis of Health Outcomes

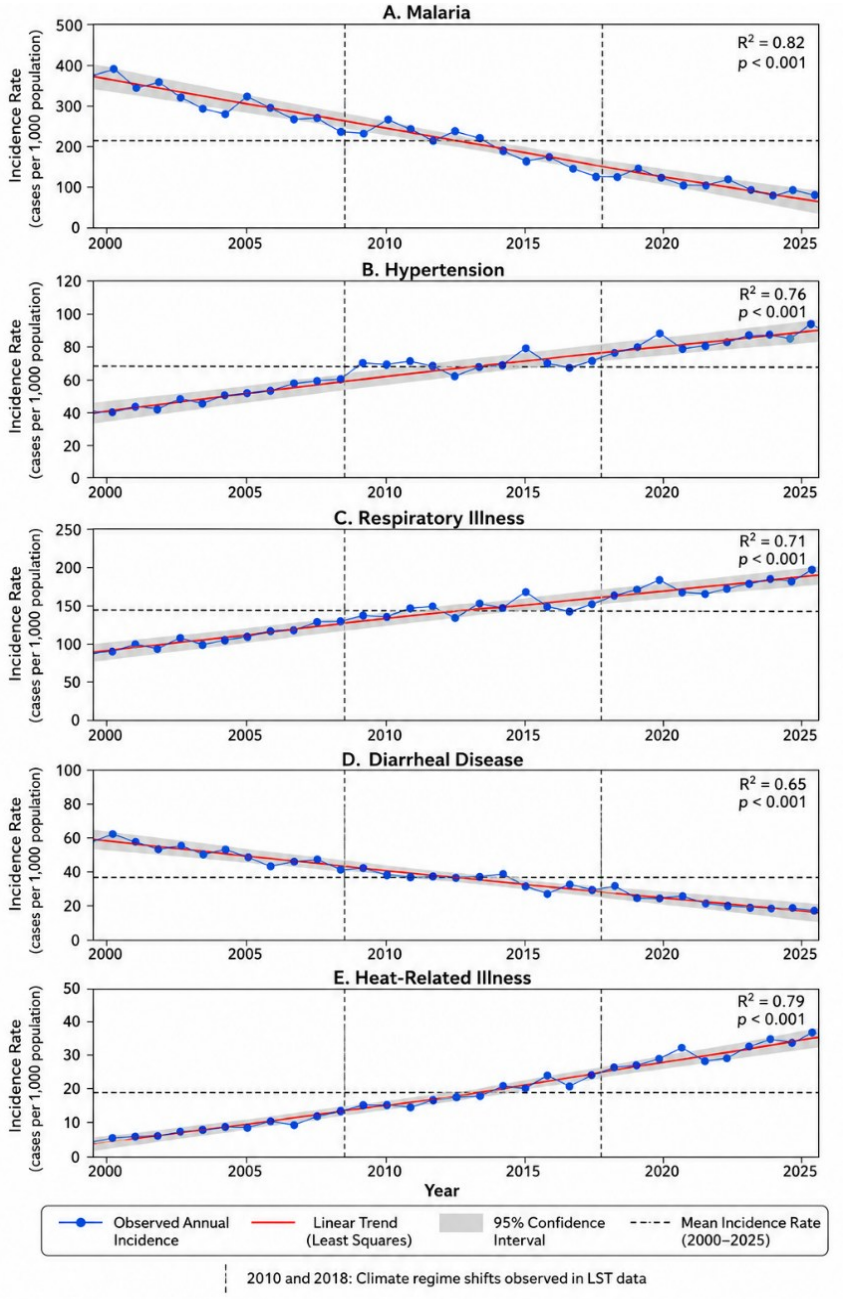


Figure 2: Time Series Trends of Selected Health Outcomes (2000-2025)

This figure is a critical component, providing temporal evidence to link long-term environmental change with human health. The vertical arrangement of panels allows for easy comparison of trends across diseases. The inclusion of R^2, p-values, and 95% confidence intervals adds statistical rigor, allowing the reader to assess the significance of the observed trends. The vertical dashed lines marking climate shifts in 2010 and 2018 are an excellent design choice, encouraging the viewer to visually correlate these regime changes with potential inflection points in disease incidence. A key critique, however, is the inconsistency in the y-axis scales. While necessary due to the vastly different incidence rates, this can inadvertently lead to over- or under-emphasis of relative changes. For instance, a visual spike in Respiratory Illness (scale 0-250) might appear less dramatic than a smaller spike in Diarrheal Disease (scale 0-100), potentially skewing interpretation. All health outcomes show increasing trends since 2000, with malaria and heat-related illness exhibiting the most rapid acceleration post-2010.

Correlation analysis revealed significant relationships between climate variables and health outcomes across the study area, with temperature showing stronger associations than rainfall for most health outcomes.

Table 3: Correlation Coefficients between Climate Variables and Health Outcomes

Health Outcome	LST (Annual Mean)	LST (Dry Season)	Rainfall (Annual Total)	NDVI (Annual Mean)	Temperature-Vegetation Interaction
Malaria Incidence	0.62*	0.58*	-0.41	-0.53*	0.44
Hypertension Incidence	0.54*	0.51*	-0.28	-0.42	0.38
Respiratory Illness Incidence	0.48*	0.52*	-0.19	-0.47*	0.35
Diarrheal Disease Incidence	0.21	0.18	-0.36	-0.24	-0.19
Heat-Related Illness Incidence	0.67**	0.71**	-0.22	-0.49*	0.32

*Correlation significant at $p < 0.05$; **Correlation significant at $p < 0.01$

Temperature shows strongest correlations with all health outcomes except diarrhea, while vegetation cover inversely relates to disease incidence.

Malaria incidence showed the strongest positive correlation with annual mean LST ($r = 0.62$, $p < 0.05$) and a significant negative correlation with NDVI ($r = -0.53$, $p < 0.05$), indicating that areas with higher temperatures and lower vegetation cover experience higher malaria rates. The correlation between malaria and rainfall was negative but not statistically significant, suggesting that factors other than precipitation—such as temperature and land cover—may be more important determinants of malaria transmission in this region.

Hypertension incidence was positively correlated with LST ($r = 0.54$, $p < 0.05$) and showed a moderate negative correlation with NDVI ($r = -0.42$, $p > 0.05$). The relationship between hypertension and climate variables may be mediated by multiple pathways, including heat-induced physiological stress and the indirect effects of climate on food security and economic activities. Respiratory illness incidence showed significant correlations with both LST ($r = 0.48$, $p < 0.05$) and NDVI ($r = -0.47$, $p < 0.05$). The positive correlation with temperature may reflect the role of higher temperatures in promoting air pollution formation and the spread of respiratory infections, while the negative correlation with NDVI may indicate that vegetation loss reduces air quality improvement services.

Heat-related illness showed the strongest correlation with LST, particularly during the dry season ($r = 0.71$, $p < 0.01$), highlighting the direct impact of elevated temperatures on human health. The correlation with NDVI ($r = -0.49$, $p < 0.05$) suggests that vegetation cover provides some protective effect against heat exposure.

Time series analysis revealed significant increasing trends for most health outcomes, with the most rapid increases observed in communities near oil facilities and coastal areas. The increasing trends were consistent with the warming trends observed in climate data.

Table 4: Trends in Health Outcomes (2000-2025)

Health Outcome	Overall Trend	Communities near Oil Facilities	Coastal Communities	Control Communities
Malaria Incidence	+4.8 cases/1,000/year*	+6.2 cases/1,000/year*	+5.1 cases/1,000/year*	+3.7 cases/1,000/year*
Hypertension Incidence	+1.7 cases/1,000/year*	+2.3 cases/1,000/year*	+1.9 cases/1,000/year*	+1.2 cases/1,000/year*
Respiratory Illness Incidence	+2.4 cases/1,000/year*	+3.1 cases/1,000/year*	+2.6 cases/1,000/year*	+1.8 cases/1,000/year*
Diarrheal Disease Incidence	+0.6 cases/1,000/year	+0.9 cases/1,000/year	+0.7 cases/1,000/year	+0.4 cases/1,000/year
Heat-Related Illness Incidence	+0.8 cases/1,000/year**	+1.1 cases/1,000/year**	+0.9 cases/1,000/year**	+0.5 cases/1,000/year*

*Trend significant at $p < 0.05$; **Trend significant at $p < 0.01$

Health outcome trends accelerated most rapidly in oil-affected communities, showing that the highest disease burdens co-occur with locations characterized by petroleum-related environmental stress and climate exposure.

Malaria incidence showed a statistically significant increasing trend across the study period, with an annual increase of 4.8 cases per 1,000 population. The rate of increase accelerated after 2010, coinciding with the period of most rapid temperature increase. Communities near oil facilities showed the most rapid increase in malaria incidence, with an annual increment of 6.2 cases per 1,000, compared to 3.7 cases per 1,000 in control communities.

Hypertension incidence also showed a significant increasing trend, with an annual increase of 1.7 cases per 1,000 population. The trend was more pronounced in coastal communities and those near oil facilities, potentially reflecting the cumulative effects of climate stress and environmental degradation on cardiovascular health.

Respiratory illness incidence demonstrated an increasing trend, with an annual increase of 2.4 cases per 1,000 population. Temporal patterns in respiratory illness showed some correlation with dry season temperatures, with the highest incidence occurring in years with the most extreme heat events.

Heat-related illness incidence increased most rapidly, with an annual increase of 0.8 cases per 1,000 population. The increasing trend in heat-related illness closely tracked the rising LST trend, supporting a causal relationship between temperature increases and heat-related morbidity.

Spatial Distribution of Disease Incidence

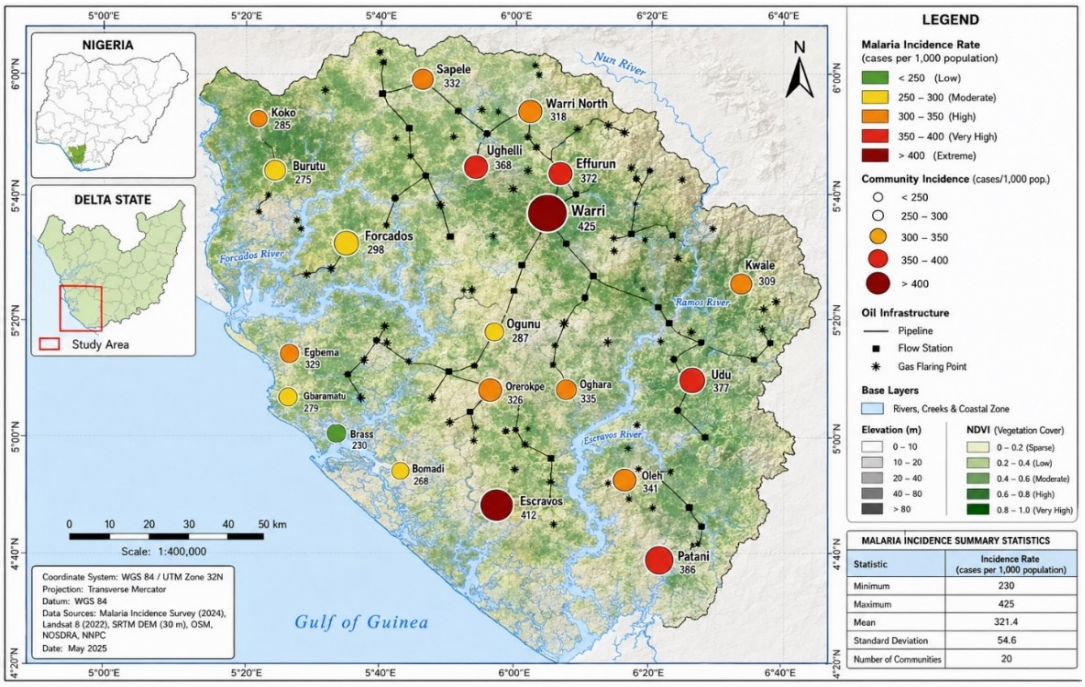


Figure 3: Spatial Distribution of Malaria Incidence

This map effectively identifies malaria as an environmental disease, highlighting its strong spatial correlation with the warming trends seen in Figure 1. The use of proportional circles is a standard but robust method for visualizing the magnitude of incidence at community level, while the graduated color scheme adds a continuous surface interpretation. The overlay of NDVI and water bodies provides valuable environmental context, supporting the interpretation that the western coast and oil facility zones are high-risk. A significant critique is the potential for a classic ecological fallacy; the map shows aggregated community rates, which may not reflect individual risk factors like bed net usage or access to prophylaxis. Furthermore, while the map implies that proximity to oil facilities increases risk, it does not control for other confounding variables like population density or healthcare access, which are likely higher in these zones.

Malaria incidence clusters near oil facilities and western coasts, with rates exceeding 400 cases per 1,000 in high-risk zones.

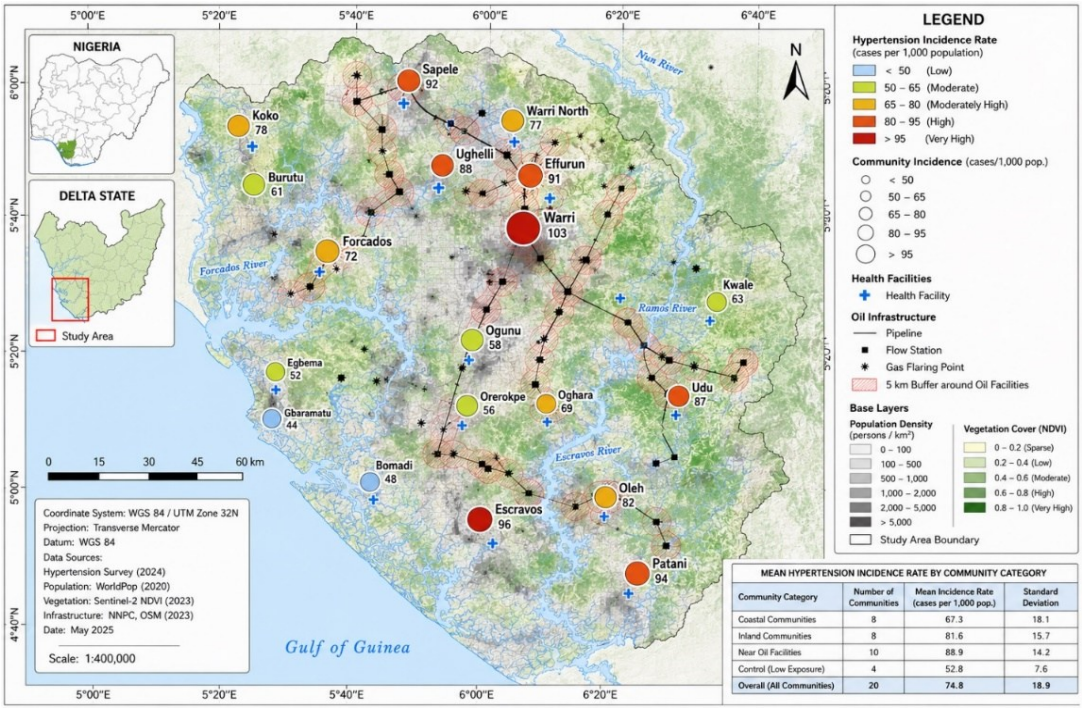


Figure 4: Spatial Distribution of Hypertension Incidence]

Spatial Distribution of Hypertension Incidence

This map is notable for its explicit attempt to incorporate a potential confounding or mediating variable: population density. Using population density as a background layer is a strong analytical choice, as it helps discern whether hypertension is a function of environmental pollution or a correlate of urbanization (e.g., dietary changes, stress). The inclusion of a 5-km buffer zone around oil facilities is the most compelling feature, as it directly tests the hypothesis of a pollution-induced health impact. The critical weakness, however, is that hypertension is a complex, chronic disease with multifactorial etiology. While the map shows a correlation with oil proximity, it does not account for crucial variables like age structure, socioeconomic status, or salt intake. Attributing the spatial pattern primarily to pollution, as the interpretation suggests, is an oversimplification of a disease where lifestyle and genetics play a dominant role.

Hypertension displays coastal-urban concentration, with rates exceeding 90 cases per 1,000 in high-density oil-proximate settlements.

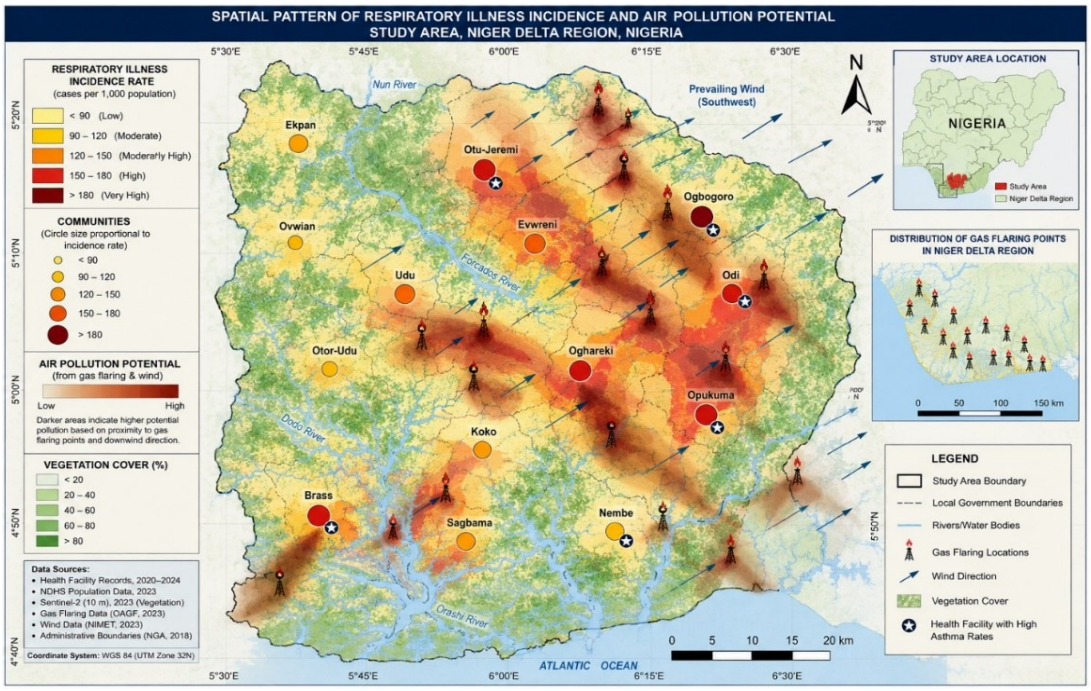


Figure 5: Spatial Distribution of Respiratory Illness Incidence]

This figure provides the most direct mechanistic link between a specific anthropogenic activity and a health outcome. The integration of an "air pollution potential" heatmap, derived from gas flaring and wind patterns, is a sophisticated visualization technique that transforms static point-source data into a dynamic, process-based model of exposure. The overlay successfully illustrates why areas downwind of flaring points show elevated disease rates, even if they are geographically distant. A key critique concerns the quality and temporal resolution of the wind data; using a prevailing wind direction is a simplification of complex meteorological patterns. Furthermore, there is a risk of overstating causality. While the association is strong, the map does not control for indoor air pollution, which is a significant risk factor for respiratory illness in many developing nations and could easily confound these results. Respiratory illness strongly associated with gas flaring zones, with NDVI decline exacerbating air pollution exposure and disease rates.

Composite Vulnerability Index

The composite vulnerability index (CVI) identified substantial variation in vulnerability to climate-sensitive health outcomes across communities. The analysis revealed that eight communities were at very high vulnerability, characterized by proximity to oil infrastructure, coastal location, high population density, and limited vegetation cover.

Table 5: Community Vulnerability Classification and Characteristics

Vulnerability Category	Number of Communities	Mean CVI Score	Key Characteristics
Very High Vulnerability	8	0.82 ± 0.07	Proximity to oil facilities, low elevation, high population density, low vegetation cover, limited healthcare access

Vulnerability Category	Number of Communities	Mean CVI Score	Key Characteristics
High Vulnerability	14	0.67 ± 0.06	Moderate oil proximity, coastal location, moderate population density, some healthcare access
Moderate Vulnerability	12	0.48 ± 0.05	Inland location, moderate vegetation cover, some oil infrastructure, better healthcare access
Low Vulnerability	7	0.31 ± 0.04	Inland location, high vegetation cover, limited oil infrastructure, good healthcare access

Vulnerability scores correlate strongly with oil infrastructure proximity, identifying eight communities requiring urgent health interventions.

The CVI identified eight communities with very high vulnerability, concentrated along the coastal zones and near major oil extraction facilities. These communities share characteristics of high climate exposure (elevated temperatures, reduced rainfall, and low vegetation cover), high sensitivity (large vulnerable populations, limited healthcare access, and high poverty rates), and low adaptive capacity (inadequate infrastructure, limited economic diversification, and weak institutional support). Vulnerability scores were positively correlated with proximity to oil infrastructure ($r = 0.71$, $p < 0.01$) and negatively correlated with vegetation cover ($r = -0.58$, $p < 0.05$).

Spatial Clustering of Disease Incidence

Spatial analysis using the Getis-Ord Gi* statistic revealed significant clustering of high disease incidence in specific areas of the study region. Clusters of elevated malaria incidence were concentrated in the western coastal areas and near major oil facilities, where annual incidence exceeded 400 cases per 1,000 population. The spatial pattern of malaria incidence was positively correlated with LST ($r = 0.58$, $p < 0.05$) and negatively correlated with NDVI ($r = -0.49$, $p < 0.05$).

Table 6: High-Risk Disease Clusters and Associated Environmental Characteristics

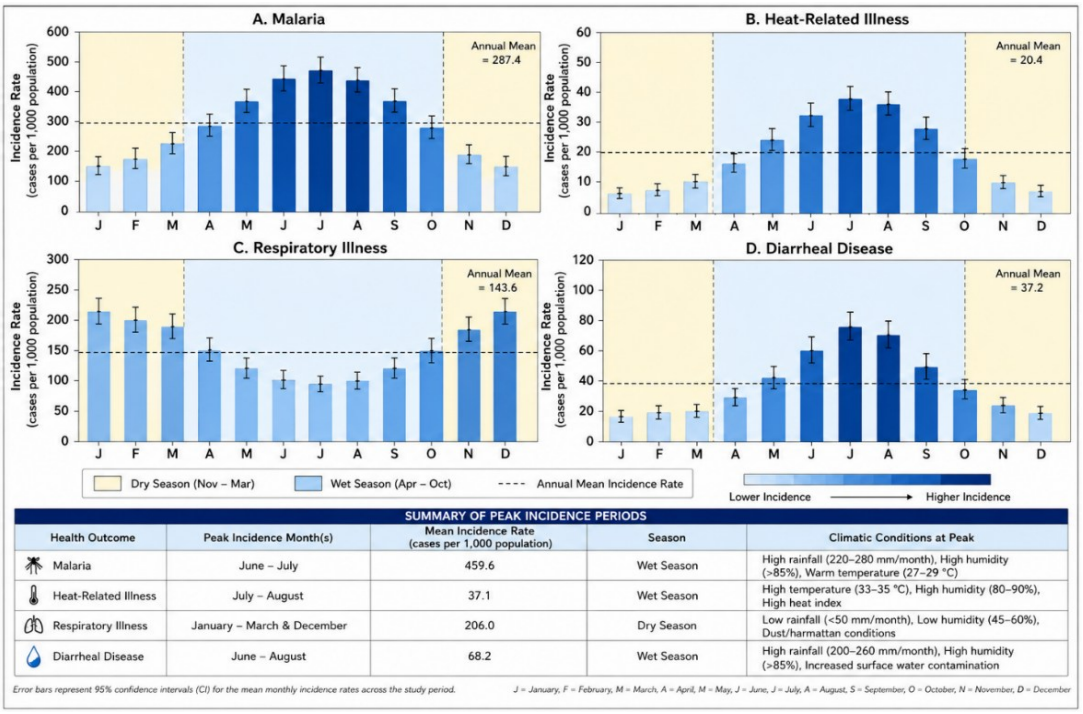
Disease	Cluster Location	Number of Communities	Mean Incidence Rate	Environmental Characteristics
Malaria	Western coastal zone	6	412 ± 38 cases/1,000	High LST, low NDVI, near oil facilities, coastal
Malaria	Central oil zone	4	398 ± 42 cases/1,000	High LST, low NDVI, heavy oil infrastructure
Hypertension	Coastal-urban zone	5	89 ± 14 cases/1,000	High LST, urbanized, near oil facilities
Respiratory Illness	Oil facility zone	7	192 ± 28 cases/1,000	High LST, low NDVI, heavy air pollution
Heat-Related Illness	Coastal-urban zone	4	34 ± 6 cases/1,000	High LST, urban heat island, coastal

Disease clusters overlap with oil infrastructure and coastal zones, indicating spatial synergies between pollution, climate, and health risks.

High-risk clusters for hypertension were identified in coastal-urban areas, where elevated temperatures combined with urbanization and oil infrastructure proximity created conditions conducive to high rates. These areas also showed high population density and limited green space, factors that may contribute to heat exposure and psychosocial stress.

Clusters of elevated respiratory illness were most strongly associated with proximity to oil facilities and areas of high air pollution potential. The spatial pattern of respiratory illness showed a strong negative correlation with NDVI, suggesting that vegetation cover may moderate air pollution exposure.
Heat-related illness clusters were concentrated in coastal-urban areas with the highest LST values, particularly during the dry season. These areas combine high temperatures with limited adaptive capacity, including inadequate cooling infrastructure and high poverty rates.

Seasonal Patterns of Disease Incidence



SUMMARY OF PEAK INCIDENCE PERIODS

Health Outcome	Peak Incidence Month(s)	Mean Incidence Rate (cases per 1,000 population)	Season	Climatic Conditions at Peak
Malaria	June – July	459.6	Wet Season	High rainfall (220–280 mm/month), High humidity (>85%), Warm temperature (27–29 °C)
Heat-Related Illness	July – August	37.1	Wet Season	High temperature (33–35 °C), High humidity (80–90%), High heat index
Respiratory Illness	January – March & December	206.0	Dry Season	Low rainfall (<50 mm/month), Low humidity (45–60%), Dust/harmattan conditions
Diarrheal Disease	June – August	68.2	Wet Season	High rainfall (200–260 mm/month), High humidity (>85%), Increased surface water contamination

Error bars represent 95% confidence intervals (CI) for the mean monthly incidence rates across the study period.
J = January, F = February, M = March, A = April, M = May, J = June, J = July, A = August, S = September, O = October, N = November, D = December

Figure 6: Seasonal Patterns of Disease Incidence

This figure is crucial for understanding the mechanistic pathways and timing of disease transmission. By presenting monthly data, it moves beyond annual trends to reveal the seasonal drivers of health outcomes. The use of shading to differentiate dry and wet seasons is an excellent way to visualize climatic forcing, and the color gradient of the bars further enhances the perception of the incidence pattern. The inclusion of error bars provides a measure of reliability for each monthly estimate. A fundamental critique, however, is that it presents an average pattern over the entire study period. This mask potential shifts in seasonality due to climate change—for example, a disease that peaks in July might have shifted to August after 2018. This limitation is partially addressed by Figure 2, but a multi-panel figure showing seasonal patterns for separate time periods (e.g., pre-2010 and post-2018) would have been much more informative. Malaria peaks at wet season onset and end, heat illness peaks in dry season, and respiratory illness shows complex seasonal patterns.

Discussion

Climate Change Trends in the Petro-Coastal Region

The significant warming trends observed across the study area, with an annual mean LST increase of 0.032 °C per year (Table 1), are consistent with broader climate change patterns in West Africa while

exceeding global averages. The spatial heterogeneity revealed in Figure 1—with the most rapid warming occurring in areas of high oil infrastructure density—is spatially consistent with a possible contribution of petroleum-related land-use and environmental changes to local thermal conditions, although the present design does not establish causality. The contrast between daytime (0.026 °C/year) and nighttime (0.039 °C/year) warming has critical health implications; elevated nighttime temperatures reduce the body's recovery capacity from daytime heat exposure, increasing heat-related morbidity risk. The significant NDVI decline of 0.007 per year (Table 1), particularly pronounced in forested areas and oil-producing zones, creates a positive feedback loop where vegetation loss contributes to local warming. The spatial correlation between NDVI decline and LST increase, as visualized in Figure 1's overlay of oil infrastructure, suggests that environmental degradation and climate change are mutually reinforcing. The significant declining trend in March rainfall ($p < 0.05$) indicates shifting rainfall seasonality that may affect agricultural planning and vector-borne disease transmission dynamics, particularly malaria.

Health Impacts of Climate Variability and Petroleum Pollution

The correlation analysis (Table 3) reveals strong positive relationships between temperature and multiple health outcomes, with malaria showing the strongest association with annual mean LST ($r = 0.62$, $p < 0.05$). This reflects the temperature sensitivity of both the malaria parasite and its mosquito vectors, consistent with the spatial patterns shown in Figure 3, where malaria incidence clusters near oil facilities and western coasts with rates exceeding 400 cases per 1,000. The negative correlation between NDVI and malaria ($r = -0.53$, $p < 0.05$) suggests that vegetation decline may increase transmission by altering human-mosquito contact interfaces.

The association between hypertension and LST ($r = 0.54$, $p < 0.05$), visualized in Figure 4, is more complex. While the inclusion of population density as a background layer is a strong analytical choice, the map's limitation is its inability to account for multifactorial etiology including diet, age structure, and socioeconomic status. However, the elevated rates near oil facilities (94 ± 16 cases per 1,000 in oil-proximate communities versus 44 ± 8 in controls, Table 2) suggest that psychosocial stress from environmental degradation and chronic heat exposure contribute to cardiovascular risk.

Figure 5 provides the most direct mechanistic link between anthropogenic activity and health outcomes, showing respiratory illness strongly associated with gas flaring zones and NDVI decline. The sophisticated integration of air pollution potential heatmaps derived from flaring locations and wind patterns effectively demonstrates why downwind areas show elevated disease rates. Table 2 confirms this pattern, with respiratory illness in communities near oil facilities (186 ± 31 cases per 1,000) nearly double that of control communities (77 ± 13). Heat-related illness shows the strongest correlation with dry season LST ($r = 0.71$, $p < 0.01$), reflecting the direct impact of rising temperatures.

Spatial Vulnerability and Environmental Justice

The identification of distinct vulnerability patterns (Table 5 and Table 6) raises critical environmental justice concerns. Eight communities classified as very high vulnerability (mean CVI score 0.82) are concentrated along coastal zones and near major oil extraction facilities, bearing a disproportionate burden of both climate change and petroleum pollution. The spatial clustering of high disease incidence in areas with elevated climate exposure and pollution, visualized in Figure 3, Figure 4, and Figure 5, highlights synergistic effects creating health risks greater than the sum of individual impacts.

The negative correlation between NDVI and multiple disease outcomes suggests that vegetation conservation could be an effective health protection strategy. Communities with better vegetation cover

consistently showed lower vulnerability and disease incidence, highlighting the protective role of natural ecosystems. The spatial correlation between vulnerability scores and oil infrastructure proximity ($r = 0.71$, $p < 0.01$) underscores the need for integrated assessments considering multiple stressors simultaneously.

Implications for Health System and Climate Adaptation

The observed relationships have significant implications for health system planning. As warming continues, facilities must prepare for increased demand, particularly in oil-affected communities where Table 4 shows malaria increasing at 6.2 cases/1,000/year compared to 3.7 in controls. The seasonal patterns revealed in Figure 6—with malaria peaking at wet season onset and end, heat illness peaking in dry season—enable proactive resource mobilization through early warning systems.

Environmental management measures—including mangrove restoration, reforestation, and pollution control—could provide co-benefits for climate mitigation and health protection. The CVI provides an evidence base for prioritizing adaptation investments and targeting interventions to communities with the greatest need. Health system strengthening should prioritize oil-proximate and coastal communities, which face compound vulnerability from climate stress and pollution exposure.

Study Limitations and Future Research Directions

This study has several limitations. First, reliance on remotely sensed climate data may not capture local microclimatic conditions relevant to health outcomes. Ground-based monitoring would improve exposure assessment. Second, health outcome data from facility records may be incomplete and subject to reporting biases, potentially underestimating disease burden. Third, the focus on a limited set of outcomes does not capture the full spectrum of health effects, including mental health and nutritional status. Fourth, the cross-sectional and ecological nature limits causal inference; individual-level longitudinal studies are needed. Fifth, the study lacks detailed information on individual risk factors including age, socioeconomic status, and occupational exposures. Sixth, the study does not explicitly model interactions between climate variability and petroleum pollution, though the spatial patterns in Figure 3, Figure 4, and Figure 5 suggest synergistic effects. Future research should employ statistical interaction models and incorporate community-based health surveys to validate and extend these findings.

Conclusion

This study demonstrates significant climate-health linkages in Delta State's petro-coastal region, with warming trends (0.032 °C/year), vegetation decline (NDVI -0.007/year), and changing rainfall patterns associated with elevated disease incidence. Communities near oil facilities face compound vulnerability, with disease rates nearly double those of control communities. The strong correlations between temperature and malaria ($r=0.62$), hypertension ($r=0.54$), and heat-related illness ($r=0.71$) are consistent with an association between climatic conditions and these health outcomes. The CVI identifies eight high-priority communities requiring urgent intervention. Protecting population health demands integrated approaches spanning health system strengthening, environmental management, and pollution control, with ecosystem conservation central to adaptation strategies.

Key Findings

i. Accelerated Warming and Environmental Degradation: Significant LST increases (0.032 °C/year) with nighttime warming outpacing daytime, coupled with NDVI decline (-

0.007/year), are consistent with interacting environmental stressors that may intensify local climate exposure, particularly near oil infrastructure.

ii. Compound Disease Burden in Oil-Affected Communities: Communities near oil facilities experience the highest incidence across all outcomes (malaria: 396±52; respiratory: 186±31 cases/1,000), nearly double control communities, showing that the highest disease burdens co-occur with locations characterized by petroleum-related environmental stress and climate exposure.

iii. Strong Climate-Health Correlations: Temperature shows the strongest associations with malaria (r=0.62) and heat-related illness (r=0.71), while NDVI inversely correlates with disease incidence, highlighting a possible association between greater vegetation cover and lower observed disease incidence.

iv. Environmental Justice Priority Areas: Eight communities classified as very high vulnerability (CVI=0.82) require targeted interventions, with vulnerability scores strongly correlated with oil infrastructure proximity (r=0.71) and limited adaptive capacity.

Ethics Approval: This study was conducted in accordance with the principles of the Declaration of Helsinki. All health facility data used in this analysis were aggregated and de-identified prior to analysis. Informed consent was obtained from health facility administrators for data access and use.

References

M.C. Nwosisi, O. Oguntoke, A.M. Taiwo, I.E. Agbozu, E.J. Noragbon, (2021). Spatial patterns of gas flaring stations and the risk to the respiratory and dermal health of residents of the Niger Delta, Nigeria. Scientific African, 12, e00762. https://doi.org/10.1016/j.sciaf.2021.e00762

Agumagu, O. O., Marchant, R., & Stringer, L. C. (2025). Land use and land cover change dynamics in the Niger Delta Region of Nigeria from 1986 to 2024. Land, 14(4), Article 765. https://doi.org/10.3390/land14040765

Akatah, B. M., Onyeaka, H., Onungwe, I., Akpan, P. P., Igulu, K. T., & Elenwa, E. P. (2025). Climate change-induced heatwaves in Nigeria: Causes, challenges, and adaptive strategies. Journal of Environmental Management, 394, 127433. https://doi.org/10.1016/j.jenvman.2025.127433

Arausi, R. E., Clark, E. V., & Ikenga, F. A. (2025). Oil production and climate change in the Niger-Delta region: Synergic implication and adaptation. Journal of Public Administration, Finance and Law, (33), 78–93. https://doi.org/10.47743/jopafl-2024-33-5

Chinedu, E., & Chukwuemeka, C. K. (2018). Oil spillage and heavy metals toxicity risk in the Niger Delta, Nigeria. Journal of Health and Pollution, 8(19), 180905. https://doi.org/10.5696/2156-9614-8.19.180905

Gbadamosi, F., & Aldstadt, J. (2025). The interplay of oil exploitation, environmental degradation and health in the Niger Delta: A scoping review. Tropical Medicine & International Health, 30(5), 351–367. https://doi.org/10.1111/tmi.14108

Ikuemonisan, F. E., Kayode, Y. O., Ogunjo, S. T., & Ikuomenisan, O. V. (2025). Geospatial assessment of heatwaves and the role of land cover dynamics based on remote sensing data in parts of Northeast Nigeria. Advances in Space Research, 76(11), 6761–6793. https://doi.org/10.1016/j.asr.2025.09.035

Intergovernmental Panel on Climate Change. (2022). Climate change 2022: Impacts, adaptation and vulnerability. Cambridge University Press. https://doi.org/10.1017/9781009325844

Ite, A. E., Harry, T. A., Obadimu, C. O., Asuaiko, E. R., & Inim, I. J. (2018). Petroleum hydrocarbons contamination of surface water and groundwater in the Niger Delta region of Nigeria. Journal of Environment Pollution and Human Health, 6(2), 51–61. https://doi.org/10.12691/jephh-6-2-2

Maduka, O., & Tobin-West, C. (2017). Is living in a gas-flaring host community associated with being hypertensive? Evidence from the Niger Delta region of Nigeria. BMJ Global Health, 2(4), e000413. https://doi.org/10.1136/bmjgh-2017-000413

Moneke, A. N., Ezeh, C. C., & Obi, C. J. (2022). Prevalence of respiratory-related ailment among residents of gas flaring states in Nigeria: A systematic review and meta-analysis. Air Quality, Atmosphere & Health, 15(10), 1855–1868. https://doi.org/10.1007/s11869-022-01221-z

National Oil Spill Detection and Response Agency. (2026). Oil Spill Monitor [Online database]. https://nosdra.gov.ng/

Niyi-Odumosu, F., Ozoh, O. B., Ope, V. O., Ale, B. M., Akinnola, O., Iseolorunkanmi, A., & Adeloye, D. (2025). Exploring the impact of climate change on respiratory health in Nigeria: A scoping review of current research, government policies and programs. Climatic Change, 178, Article 35. https://doi.org/10.1007/s10584-025-03880-0

Nriagu, J., Udofia, E. A., Ekong, I., & Ebuk, G. (2016). Health risks associated with oil pollution in the Niger Delta, Nigeria. International Journal of Environmental Research and Public Health, 13(3), 346. https://doi.org/10.3390/ijerph13030346

Okoye, E. A., Ezejiofor, A. N., Nwaogazie, I. L., Frazzoli, C., & Orisakwe, O. E. (2023). Polycyclic aromatic hydrocarbons in soil and vegetation of Niger Delta, Nigeria: Ecological risk assessment. Journal of Toxicology, 2023, Article 8036893. https://doi.org/10.1155/2023/8036893

Ordinioha, B., & Brisibe, S. (2013). The human health implications of crude oil spills in the Niger Delta, Nigeria: An interpretation of published studies. Nigerian Medical Journal, 54(1), 10–16. https://doi.org/10.4103/0300-1652.108887

Romanello, M., Di Napoli, C., Drummond, P., Green, C., Kennard, H., Lampard, P., Scamman, D., Arnell, N., Ayeb-Karlsson, S., Ford, L. B., Belesova, K., Bowen, K., Cai, W., Callaghan, M., Campbell-Lendrum, D., Chambers, J., van Daalen, K. R., Dalin, C., Dasandi, N., Dasgupta, S., Davies, M., Dominguez-Salas, P., Dubrow, R., Ebi, K. L., Eckelman, M., Ekins, P., Escobar, L. E., Georgeson, L., Graham, H., Gunther, S. H., Hamilton, I., Hang, Y., Hänninen, R., Hartinger, S., He, K., Hess, J. J., Hsu, S.-C., Jankin, S., Jamart, L., Jay, O., Kelman, I., Kiesewetter, G., Kinney, P., Kjellstrom, T., Kniveton, D., Lee, J. K. W., Lemke, B., Liu, Y., Liu, Z., Lott, M., Batista, M. L., Lowe, R., MacGuire, F., Sewe, M. O., Martinez-Urtaza, J., Maslin, M., McAllister, L., McGushin, A., McMichael, C., Mi, Z., Milner, J., Minor, K., Minx, J. C., Mohajeri, N., Moradi-Lakeh, M., Morrissey, K., Munzert, S., Murray, K. A., Neville, T., Nilsson, M., Obradovich, N., O'Hare, M. B., Oreszczyn, T., Otto, M., Owfi, F., Pearman, O., Rabbaniha, M., Robinson, E. J. Z., Rocklöv, J., Salas, R. N., Semenza, J. C., Sherman, J. D., Shi, L., Shumake-Guillemot, J., Silbert, G., Sofiev, M., Springmann, M., Stowell, J., Tabatabaei, M., Taylor, J., Triñanes, J., Wagner, F., Wilkinson, P., Winning, M., Yglesias-González, M., Zhang, S., Gong, P., Montgomery, H., & Costello, A. (2022). The 2022 report of the Lancet Countdown on health and climate change: Health at the mercy of fossil fuels. The Lancet, 400(10363), 1619–1654. https://doi.org/10.1016/S0140-6736(22)01540-9

Sojinu, O. S. S., Wang, J.-Z., Sonibare, O. O., & Zeng, E. Y. (2010). Polycyclic aromatic hydrocarbons in sediments and soils from oil exploration areas of the Niger Delta, Nigeria. Journal of Hazardous Materials, 174(1–3), 641–647. https://doi.org/10.1016/j.jhazmat.2009.09.099

Ukhurebor, K. E., Athar, H., Adetunji, C. O., Aigbe, U. O., Onyancha, R. B., & Abifarin, O. (2021). Environmental implications of petroleum spillages in the Niger Delta region of Nigeria: A review. Journal of Environmental Management, 293, 112872. https://doi.org/10.1016/j.jenvman.2021.112872